ASSOCIATION OF THE T-TYPE $Ca_V3.2$ (α_{1H}) VSCC WITH THE AUXILIARY $\alpha_2\delta_1$ SUBUNIT IN MLO-Y4 CELLS

by

Amber S. Majid

A thesis submitted to the Faculty of the University of Delaware in partial fulfillment of the requirements for the degree of Honors Bachelor of Arts in Biological Sciences with Distinction.

Spring 2009

ASSOCIATION OF THE T-TYPE $Ca_V3.2$ (α_{1H}) VSCC WITH THE AUXILIARY $\alpha_2\delta_1$ SUBUNIT IN MLO-Y4 CELLS

by

Amber S. Majid

Approved: _____

Mary C. Farach-Carson, Ph.D.
Professor in charge of thesis on behalf of the Advisory Committee

Approved: _____

Kirk J. Czymmek, Ph.D.
Committee member from the Department of Biological Sciences

Approved: _____

Marlene G. Emara, Ph.D.
Committee member from the Board of Senior Thesis Readers

Approved: _____

Alan D. Fox, Ph.D.
Director, University Honors Program

ACKNOWLEDGMENTS

First and foremost, I would like to thank Dr. Farach-Carson for giving me the opportunity to work in her lab since I was a sophomore. She paired me with William Thompson, who has made my undergraduate research experience a challenging and worthwhile part of my college career.

This project would not have been possible without the generous donation of the MLO-Y4 cell line by Dr. Lynda Bonewald and the $\alpha_2\delta_1$ antibody by Dr. Jesus Garcia.

I would also like to thank the other members of both the Farach-Carson and Carson labs who have shown support and interest in my project. Additionally, I would like to express gratitude to my family for their infinite patience and understanding. Finally, I would like to express my personal thanks to Cath Weissman, Richard Duong, Eric Mojica, Aivi Nguyen, and Ritika Samant.

TABLE OF CONTENTS

LIST OF TABLES

LIST OF FIGURES

LIST OF ABBREVIATIONS

BSA	bovine serum albumin
BTZ	benzothiazepines
DHP	dihydropyridine
DMP-1	dentin matrix protein 1
DT	diphtheria toxin
E11	podoplanin
ECM	extracellular matrix
EDTA	ethylene diamine tetraacetic acid
FBS	fetal bovine serum
GK	guanylate kinase
HRP	horseradish-peroxidase
HVA	high-voltage activated
LVA	low-voltage activated
MAGUK	membrane-associated guanylate kinase
M-CSF	macrophage colony-stimulating factor
MEPE	matrix extracellular phophoglycoprotein with ASARM motif
MLO-Y4	murine-long bone osteocyte-Y4 line
mRNA	messenger RNA
NO	nitric oxide
OPG	osteoprotegerin
PAA	phenylalkylamines
PBS	phophate buffered saline
PDZ	postsynaptic density-95 (PSD-95)/Dlg/ZO-1
RANK	receptor activator of nuclear factor κB
RANKL	receptor activator of nuclear factor κB ligand
RT-PCR	reverse transcriptase polymerase chain reaction
SEB	sample extraction buffer
SH3	Src-Homology-3
SNARE	soluble NSFattachment protein receptors
TAE	Tris Acetate-EDTA
TBS	tris-buffered saline
TCA	trichoroacetic acid
TGF	transforming growth factor
TME	total mouse embryo
VSCC	voltage sensitive calcium channel
VWA	von Willebrand factor type A

ABSTRACT

Bone contains three major cell types: bone-forming osteoblasts, bone-resorbing osteoclasts, and osteocytes, which are terminally differentiated osteoblasts embedded in mineralized matrix. Osteocytes communicate with one another through dendrite-like processes extending from cell bodies. While their function is not completely understood, osteocytes sense mechanical signals within bone and translate these signals into responses by effector cells. Voltage sensitive calcium channels (VSCCs) span the cell membrane and open in response to external stimuli resulting in altered Ca^{2+} permeability. Once inside the cell, Ca^{2+} acts as a second messenger eliciting specific cellular responses. L-type VSCCs are composed of a complex of polypeptide units consisting of a pore forming α_1 subunit, an intracellular β subunit, a dimer of disulfide linked $\alpha_2\delta$ subunits, and a transmembrane γ subunit in some tissues, but not in osteoblasts. While osteoblasts predominantly express L-type $Ca_v1.2$ (α_{1C}) VSCCs, osteocytes have been shown to express mainly T-type $Ca_v3.2$ (α_{1H}) subunit. Expression of auxiliary VSCC subunits never has been studied in osteocytes, and furthermore, the association of auxiliary subunits with T-type VSCC subunits never has been demonstrated in bone or any other tissue. The goal of this study was to elucidate the expression profile of VSCC subunits in osteocytes and to demonstrate an association of the extracellular auxiliary $\alpha_2\delta$ subunit and the $Ca_v3.2$ subunit. Using RT-PCR, Western

blot, and immunostaining, I demonstrated that the T-type $Ca_v3.2$ (α_{1H}) subunit is the predominant α_1 subunit of MLO-Y4 cells. Additionally, MLO-Y4 cells express $\alpha_2\delta_1$, γ_7, and β_{1-3} subunits at the transcript level. Co-immunoprecipitation assays demonstrated the presence of an association between $Ca_v3.2$ (α_{1H}) and the $\alpha_2\delta_1$ auxiliary subunit. This association can stabilize the functional channel, and provide a mechanism of interaction with the extracellular environment. This key protein complex may provide a crucial function for mechnanosensitive osteocytes in bone, having implications in skeletal remodeling and osteoporosis.

Chapter 1

INTRODUCTION

1.1 Osteoporosis is a rising health concern

Osteoporosis, a disease characterized by microarchitectural deterioration of bone, most often leads to increased bone fragility and susceptibility to fracture (Cooper, 1999). While 10 million Americans over the age of 50 have osteoporosis, another 34 million people are at risk for developing this skeletal disease (Cooper, 1999). With life expectancy increasing globally, and the elderly population on the rise, osteoporosis is a rising concern for future generations (Holroyd et al., 2008).

Osteoporotic fractures lead to severe mortality and morbidity at a cost of approximately $17.9 billion a year in the United States (Cooper, 1999). Hip and vertebral fractures, in particular, have been associated with excessive mortality with about 740,000 deaths per year resulting from complications of hip fractures (Johnell and Kanis, 2006). Additionally, of those individuals initially hospitalized for hip fractures, 8% of men and 3% of women over the age of 50 die, and one year post fracture, these rates rise to of 36% for men and 21% for women (Cooper, 1999).

Not only do osteoporotic fractures pose a burden on society, but they also impart a large economic cost. It is predicted that the cost of osteoporosis related

fractures to the US healthcare system will rise to $50 billion by the year 2040 (Miller, 1999). The expense associated with osteoporosis is growing faster than the general inflation rate, thus imposing a significant alert to many countries (Cummings and Melton, 2002). While there has been a great deal of progress made in the development of therapies and rehabilitation programs for osteoporotic individuals, the potential for more specific and effective treatments depends on the expansion of current bone research and a collaborative effort between scientists and clinicians.

1.2 Bone is composed of several cell types

Bone, a specialized connective tissue, consists of a variety of cell types, a calcified extracellular matrix, and extracellular fluid (Cummings and Melton, 2002, Aarden et al., 1994). This system, organized hierarchically, functions to protect and support organs and tissues, to serve as a reserve for calcium, phosphate, and magnesium, and to maintain the homeostasis of those ions (Aarden et al., 1994). As a living and self-renewing tissue, bone is constantly adapting to changes in the environment, an attribute that is controlled by an intricate balance in the activities of several cell types including osteoblasts, osteoclasts, and osteocytes (Aarden et al., 1994).

Osteoblasts, derived from mesenchymal stem cells, produce new bone through the synthesis and secretion of osteoid, an unmineralized bone matrix composed of type I collagen and other noncollagenous proteins such as osteocalcin,

osteopontin, and osteonectin (Katagiri and Takahashi, 2002). At different growth phases, osteoblasts exhibit specific patterns of gene expression (Lian and Stein, 1995). Their stages of differentiation are marked by a number of phenotypic markers including alkaline phosphatase, cytokines, and bone-matrix proteins like fibronectin (Stein et al., 1990).

Osteoclasts, derived from hematopoietic cells, are positioned on the bone surface and play an important role in the resorption of bone matrix (Ash et al., 1980). The apical surface of osteoclasts attach to bone matrix via integrins to form the sealing zone, which is characterized by the presence of a ruffled border, the term used to describe deep folds of the plasma membrane (Davies et al., 1989). Osteoclasts pump large amounts of H^+ into the sealed resorption zone and acidify the extracellular fluid to dissolve hydroxyapatite. They also secrete cathepsin K and tartrate-resistant acid phosphatase into the bone-resorbing compartment (Vaananen et al., 2000). These lysozomal enzymes, in addition to other proteases, hydrolyze collagen and release extracellular matrix (ECM)-trapped growth factors, like insulin growth factor and transforming growth factor-β (TGF-β) (Blair, 1998).

Osteocytes are the most abundant cell type in bone, making up over 90% of all bone cells (Marotti et al., 1995). They are terminally differentiated osteoblasts. Once the osteoid begins to mineralize, some osteoblasts become trapped in the matrix and become osteocytes, while others become flat bone-lining cells (Wang et al., 1999). Those osteoblasts that become osteocytes lose many of their cellular organelles and

cytoplasmic volume, transforming from a large cuboidal conformation to a stellate shaped morphology. This stellate morphology is characterized by the presence of long, slender dendrite-like processes radiating from the cell body (Figure 1). Osteocyte cell bodies are surrounded by mineralized matrix and the space between the cell body and the matrix are known as lacunae, while the processes extend into channels called canaliculi. These cytoplasmic extensions are essential in transporting nutrients to, and wastes away from the cells in the extracellular space (Aarden et al., 1994). In contrast, gap junctions located on osteocyte processes allow for communication via intracellular ion transport among osteocytes, osteoblasts, and the more superficially located bone lining cells. This functional syncytium, composed of multiple cell types, works as an interconnected network due to the presence of common surroundings; a continuous, fluid-filled, proteoglycan-rich space (Knothe Tate, 2003).

The understanding of osteocyte physiology lags behind that of other bone cell types largely because these cells are difficult to access due to the surrounding mineralized matrix. For this reason, several osteocyte cell lines have been generated, of which the murine long bone osteocyte-Y4 (MLO-Y4) line was created by Dr. Lynda Bonewald (University of Missouri-Kansas City, Kansas City, MO). The MLO-Y4 cell line was created by the extraction of osteocytes from transgenic mice expressing the SV40 large T-antigen using the osteocalcin promoter. MLO-Y4 osteocyte-like cells are characterized by low alkaline phosphatase and collagen type I expression and relatively higher levels of osteocalcin, connexin 43, and E11 (Bonewald, 1999).

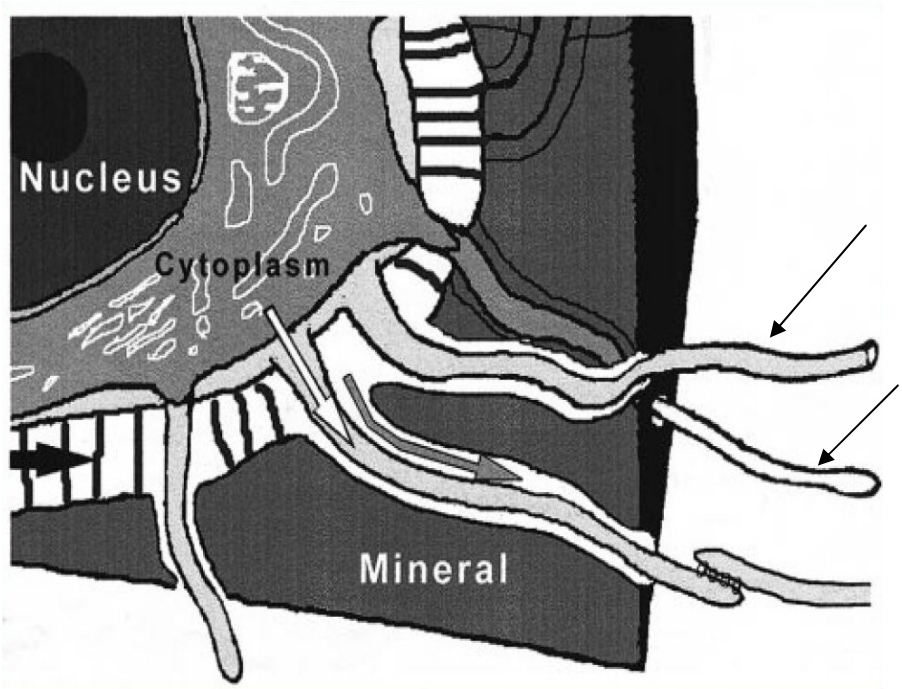

Figure 1: The osteocyte cell processes, located within fluid filled, proteoglycan rich canalicular spaces, allow for osteocytes to interact with one another as well as to bone lining cells (Bonewald, 1999).

1.3 Bone remodeling: a well orchestrated balance of cellular activities

Bone remodeling involves a balance between bone resorption and formation, and involves three steps, resorption, reversal, and formation (Hadjidakis and Androulakis, 2006). The first step in this remodeling process begins with the activation of osteoclastic precursors by cells of the osteoblastic lineage. The activating cells change physically and secrete enzymes that function at the bone surface to digest protein. They also express receptor activator of nuclear factor-kappa B ligand (RANKL), a 317 amino acid long polypeptide and member of the tumor necrosis factor superfamily (Hadjidakis and Androulakis, 2006). Osteoclast precursors contain the transmembrane receptor activator of nuclear factor-kappa B (RANK), and the resulting interaction between RANK and RANKL serves to activate and fuse hematopoietic cells to osteoclastic cells to begin resorption (Hadjidakis and Androulakis, 2006).

Osteoclastogenesis is also promoted by macrophage colony-stimulating factor (M-CSF). This molecule functions by binding to c-Fms, its receptor, which is located on osteoclast precursors (Udagawa et al., 1990). In order for osteoclastogenesis to occur, there must be interaction between osteoclast precursors and stromal cells or osteoblasts. Osteoprotegerin (OPG), a surface-residing molecule that competes with RANK for RANKL is a necessary element of osteoclastogenesis (Lacey et al., 1998). OPG blocks the receptor-ligand interaction and neutralizes the function of the ligand.

The quantity of bone that is resorbed depends on the exact ratio between RANKL and OPG (Hofbauer et al., 1999).

1.4 Osteocytes function as the mechanosensors of bone

Due to the deep location of osteocytes within mineralized tissue, studies to determine their exact function have been limited and difficult. Osteocytes are thought to be the primary mechanosensor cells of bone, but the precise mechanism by which they sense strain is incompletely understood. Osteocytes are well positioned in bone to sense mechanical strain. They translate that signal by a currently unknown mechanism, into a biochemical response which can be signaled to bone effector cells. In response to stress, these cells regulate bone mass (Figure 2). The translated forces, whether biochemical or electrochemical, occur in the pericellular fluid which is the coupling medium that lies within the lacunocanalicular system (Knothe Tate, 2003).

Mechanical strain is known to regulate osteoclast and osteoblast activity. Osteoblasts themselves, in addition to osteocytes, are physiologically able to sense mechanical strain. However, of these cell types, osteocytes, due to their high population and morphology in bone, are thought to be the primary cell type to sense and translate strain (Lanyon, 1993). One proposed mechanism to account for the mechanosensitive properties of osteocytes is the direct deformation of the cell membrane as a result of fluid shear stress within the lacunocanalicular system of bone (Weinbaum et al., 1994).

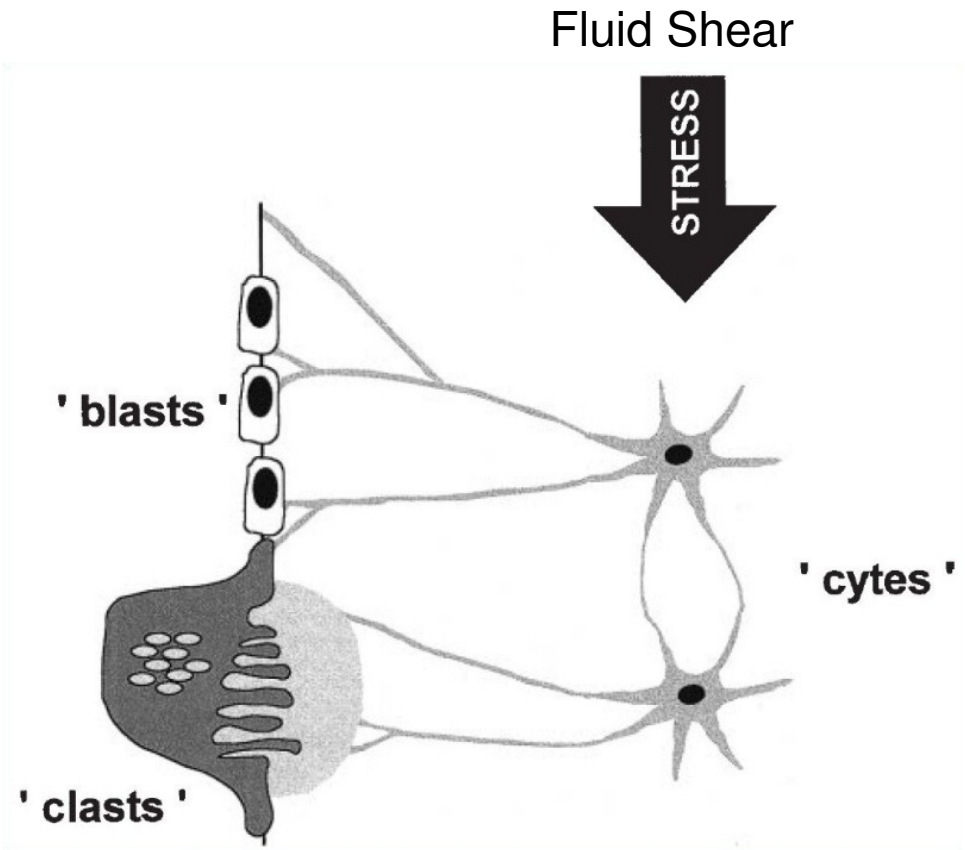

Figure 2: The interconnected network existing between osteocytes, osteoblasts, and osteoclasts is important in considering the transmission of mechanical stresses on bone (Bonewald, 1999).

There is strong evidence to support the proposed role of osteocytes as mechanosensors of bone. Skerry and colleagues demonstrated increased expression of glucose 6-phosphate dehydrogenase in osteocytes within minutes after loading bone (Skerry et al., 1989). Additionally, c-Fos transcript is upregulated in osteocytes after two hours of loading, and by four hours, mRNA levels of insulin-like growth factor-1 and growth factor-β have increased as well (Raab-Cullen et al., 1994). Other markers, such as E11/gp38, dentin matrix protein 1 (DMP-1), matrix extracellular phosphoglycoprotein with ASARM motif (MEPE), and sclerostin also exhibit changes in expression levels after bone loading (Gluhak-Heinrich et al., 2003, Zhang et al., 2006). Osteocytes also secrete anabolic signals such as nitric oxide (NO), prostaglandins, and ATP after loading (Ajubi et al., 1999, Bakker et al., 2001). Additionally, Tatsumi and colleagues found that specific ablation of osteocytes with diphtheria toxin (DT) killed approximately 70% to 80% of osteocytes. The osteocyte null mice resisted unloading-induced bone loss, supporting the notion of a mechanotransductive role for osteocytes (Tatsumi et al., 2007).

1.5 VSCCs regulate the mechanical response of bone cells

VSCCs are essential for cellular functions, such as muscle contraction and neurotransmitter release (Dolphin, 1995). These channels mediate the intracellular concentration of calcium ions in response to membrane depolarization, protein phosphorylation events, or G protein signaling cascades (Catterall, 2000). Ca^{2+} acts as

a second messenger, affecting a number of intracellular processes such as the activity of Ca^{2+}-sensitive enzymes and gene expression. VSCCs are classified by specific characteristics and grouped into one of five subtypes, including L-, N-, P/Q-, R-, and T-types (Catterall, 2000). These subtypes can be further grouped based on their activation potential. High-voltage activated (HVA) channels, including the P/Q-, N-, R-, and L-types, are stimulated by strong depolarizations, while low-voltage activated (LVA) channels, including the T-types, are triggered by lower depolarizations (Table 1).

HVA channels in excitable cells such as muscle are composed of several subunits including α_1, β, $\alpha_2\delta$, and γ (Figure 3) (Catterall, 2000). Of the four distinct L-type channels, $Ca_v1.2$ (α_{1C}) predominantly is expressed in growth phase osteoblasts (Meszaros et al., 1996). This channel is fully functional and responds to changes in membrane potential (Caffrey and Farach-Carson, 1989). Osteoblasts contain the α_1 subunit, an intracellular β subunit, the auxiliary $\alpha_2\delta$ subunit, but no γ subunit (Bergh et al., 2004). T-type channels, which are key in skeletal growth, inactivate much faster than HVA channels, conduct transient current, and show a low affinity to HVA antagonists and have been implicated in cardiac pacemaker and thalamic neuron activity (Perez-Reyes et al., 1998, Shao et al., 2005). While the auxiliary subunit composition HVA VSCCs has been well-defined, the association of auxiliary subunits with the T-type channel has never been definitively demonstrated in bone or any other tissue (Perez-Reyes, 2006).

1.5.1 α_1 subunit

The α_1 subunit is the pore-forming subunit of the VSCC complex and is necessary for channel function serving as the site for the binding of channel blockers. A functional channel may form with only the α_1 subunit, but it lacks key regulatory functions (Perez-Reyes et al., 1989).

The molecular weight of the α_1 subunit is 190kD to 250kD and contains four repeat domains (I to IV) linked to one another by cytoplasmic loops. Each domain contains six membrane spanning regions, S1 to S6 (Catterall, 2000). The membrane-associated loop between S5 and S6 forms the pore lining region. The S4 segments contain positively charged lysine and arginine residues, which form the voltage sensor that results in a conformational change in response to membrane depolarization (Catterall, 2000). There are ten genes of the α_1 subunit, each one expressed differently in various tissues.

The L-type or Ca_v1 family of calcium channels, namely α_{1C}, α_{1D}, α_{1F}, and α_{1S}, inactivate slowly. They are the predominant VSCCs found in muscle, endocrine, and neuronal cells and are regulated by protein phosphorylation mediated by kinase pathways (Catterall, 2000). L-type VSCCs are blocked by dihydropyridines (DHPs), phenylalkylamines (PAAs), and benzothiazepines (BTZs), which function by binding to the S6 region.

The remainder of the high-voltage activated channels, the Ca_v2 family, differ from the Ca_v1 family in terms of regulation. These channels are controlled by direct

Table 1: Nomenclature, localizations, channel blockers, and function of different types of Ca^{2+} channels (Catterall, 2000, Bergh et al., 2003)

Ca^{2+} channel	Ca^{2+} current type	Primary Localizations	Previous names	Functions
$Ca_v1.1$	L	Skeletal Muscle	α_{1S}	Excitation-contraction coupling
				Calcium homeostasis
				Gene Regulation
$Ca_v1.2$	L	Cardiac Muscle	α_{1C}	Excitation-contraction coupling
		Endocrine Cells		Hormone Secretion
		Neurons		Gene Regulation
		Osteoblasts		
$Ca_v1.3$	L	Endocrine Cells	α_{1D}	Hormone Secretion
		Neurons		Gene Regulation
$Ca_v1.4$	L	Retina	α_{1F}	Tonic neurotransmitter release
$Ca_v2.1$	P/Q	Nerve Terminals	α_{1A}	Neurotransmitter Release
		Dendrites		Dendritic Ca^{2+} transients
$Ca_v2.2$	N	Nerve Terminals	α_{1B}	Neurotransmitter Release
		Dendrites		Dendritic Ca^{2+} transients
$Ca_v2.3$	R	Cell Bodies	α_{1E}	Ca^{2+}-dependent action potentials
		Dendrites		
		Nerve Terminals		Neurotransmitter Release
$Ca_v3.1$	T	Cardiac Muscle	α_{1G}	Repetitive ring
		Skeletal Muscle		
		Neurons		
$Ca_v3.2$	T	Cardiac Muscle	α_{1H}	Repetitive ring
		Neurons		
$Ca_v3.3$	T	Neurons	α_{1I}	Repetitive ring

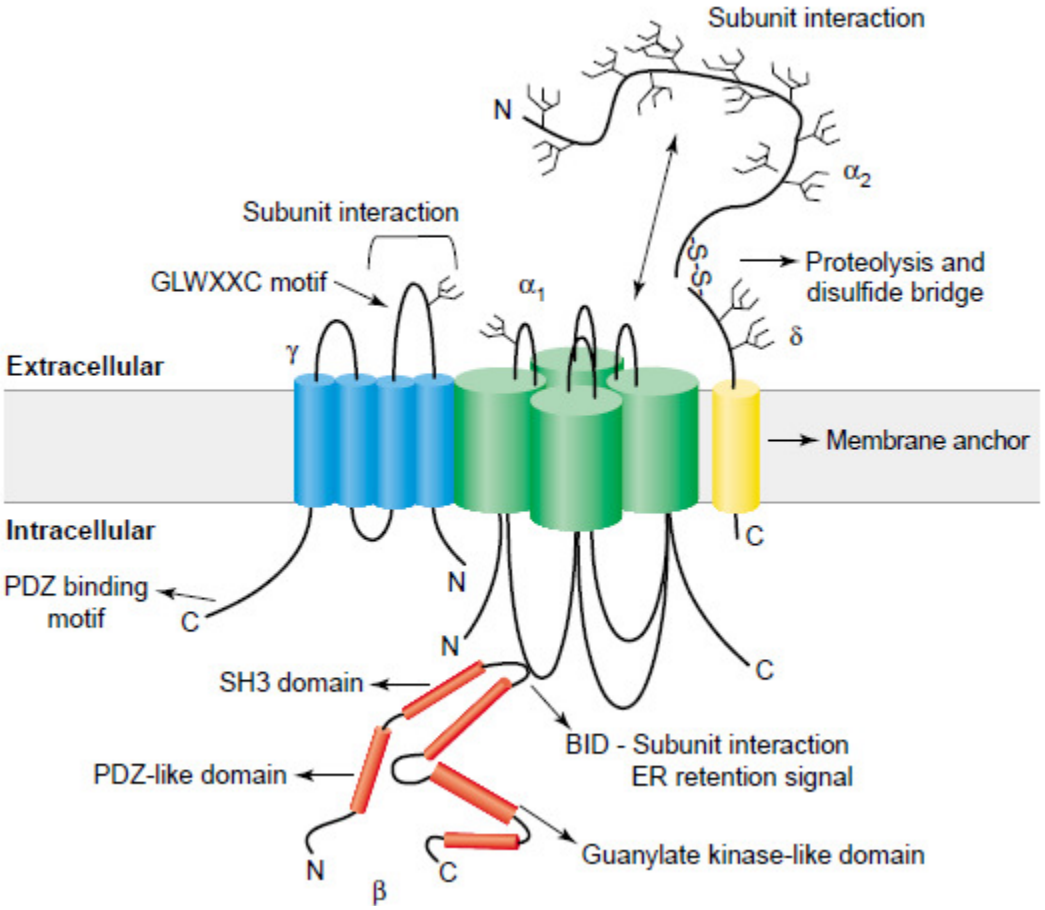

Figure 3: Structural Organization of voltage-gated calcium channels (Arikkath and Campbell, 2003)

binding of SNARE proteins and G proteins and mainly are found in neurons, differing only in the identity of the toxin blocker, which is snake or spider venom.

Finally, the Ca_v3 family, known also as T-type channels, differ from the Ca_v1 and Ca_v2 families in that it is a LVA family, with transient activation. They are found in a variety of cell types and assist with neuronal firing, muscle contraction, and hormone secretion (Perez-Reyes, 2003). Shao and colleagues demonstrated that osteocytes primarily express the T-type, $Ca_v3.2$ (α_{1H}) subunit compared to the L-type, $Ca_v1.2$ (α_{1C}) subunit found in osteoblasts, the precursors of osteocytes (Shao et al., 2005, Bergh et al., 2003).

1.5.2 $\alpha_2\delta$ subunit

Genes encoding four $\alpha_2\delta$ subunits have been identified (Burgess et al., 2001). While membrane topology for the $\alpha_2\delta$ subunit first was found for skeletal muscle $\alpha_2\delta_1$, all four subunits demonstrate a similar structure (Gurnett et al., 1996, Gurnett et al., 1997). They are all type I transmembrane proteins with an extracellular N-terminal signal sequence and a C-terminal hydrophobic region. Early research on the $\alpha_2\delta$ subunit showed that the α_2 subunit is completely extracellular and disulfide-bonded to the transmembrane δ subunit to form a dimer of 175 kDa (Jay et al., 1991). This subunit is the product of a single gene, and is post-translationally glycosylated and proteolytically cleaved once the intra-subunit disulfide bond is formed (Catterall, 2000). Glycosylation is integral in maintaining the interaction between the $\alpha_2\delta$ and α_1

subunit (Gurnett et al., 1997). Tissue expression of the $\alpha_2\delta$ subunit varies among each of the four subunits. The $\alpha_2\delta_1$ transcript and protein is highly expressed in skeletal muscle and other tissues (Ellis et al., 1988, Gong et al., 2001).

Three domains have been identified for the $\alpha_2\delta$ subunit. The first is the von Willebrand factor type A (VWA) domain. It is present in the extracellular sequence of the $\alpha_2\delta$ subunit and has been shown to regulate collagen and factor VIII binding in von Willebrand factor. The remaining two are Cache domains, one of which immediately follows the VWA domain (Anantharaman and Aravind, 2000). These domains bind to small-molecule ligands like amino acids. The extracellular α_2 region of $\alpha_2\delta$ interacts with the α_1 subunit at the third transmembrane domain of α_1. Due to the inability of the α_1 transmembrane domain to completely regulate the interaction, secondary interaction sites may exist.

$\alpha_2\delta$ function can be influenced by the presence of the β subunit. The $\alpha_2\delta$ subunit increases the VSCC current in addition to altering the activation and inactivation kinetics of the α_1 subunit (Arikkath and Campbell, 2003, Klugbauer et al., 2003). These current effects rely upon the large number of glycosylation sites located on the $\alpha_2\delta$ subunit. The presence of $\alpha_2\delta$ also has been shown to increase the number of DHP binding sites on VSCCs (Klugbauer et al., 2003).

1.5.3 β subunit

The intracellular β subunit is between 52kDa and 77kDa and is known to interact with the α_1 subunit through its cytoplasmic loop. There are four distinct genes encoding for four distinct β subunits, (β_{1-4}), each having a number of splice variants (Helton and Horne, 2002). The different β subunits can have variable effects on channel kinetics and gating characteristics. For example, compared with β_3 activity, β_2 expression in cardiac tissue leads to larger currents and more rapid gating through the L-type VSCC (Hullin et al., 2003). All four of the subunits are expressed in brain with differential expression in other tissues. There is a great functional diversity associated with calcium channels, usually attributed to the ten α_1 subunits; but the interaction between the α_1 and β subunits confers an even greater diversity (Liu et al., 1996).

The β subunit can influence voltage dependence of activation, inactivation characteristics, peak current amplitude, and channel trafficking to the plasma membrane (Catterall, 2000). It targets the α_1 subunit to the plasma membrane, a function which may be influenced through the palmitoylation of the N-terminus for the β_{2a} subunit based on previous findings demonstrating that palmitoylation localizes other proteins to lipid rafts on the plasma membrane (Dolphin, 2003, Resh, 1999). For other β subunit targeting to occur, palmitoylation is not required (Gao et al., 1999).

The β subunit is composed of five domains, two conserved regions, D2 and D4, and three variable motifs, D1, D3 and D5 (De Waard et al., 1994). Protein analysis has shown great similarity between the membrane-associated guanylate kinase

(MAGUK) proteins and the β subunit. MAGUK proteins function to cluster ion channels, receptors, and organize intracellular signaling pathways (Betanzos et al., 2004). Like MAJUK, the β subunit contains a Src-Homology-3 (SH3) region, a guanylate kinase-like (GK) domain, and a postsynaptic density-95 (PSD-95)/disc large/zona occludens (PDZ) domain (Sheng and Pak, 2000). The SH3 motif is present in D2, and between the D3 and D4 domains, is the BID. D4 contains the GK domain, and a PDZ domain is present in the N-terminal sequence, although it is not conserved. While the variable regions provide each β subunit with distinct function, the conserved regions supply a common function to all β subunits (Takahashi et al., 2004).

Interaction between the α_1 and β subunits occurs at the I-II intracellular loop through a conserved sequence, with binding on the α interaction domain (AID) of the α subunit and on the β interaction domain (BID) of the β subunit (De Waard et al., 1994, Pragnell et al., 1994). When a mutated AID exists, membrane trafficking and binding between β and α_1 is affected (Arikkath and Campbell, 2003). Although there is great flexibility when considering the pairing between α_1 and β, each calcium channel does have a preferred β subunit. For example, for the P/Q-type channels, β_4 is usually preferred, while β_3 is typically favored for the N-type channels. Finally, VSCC activity can be modulated by phosphorylating the β subunit in two possible sites on the D3 linker region (Takahashi et al., 2004). In osteoblastic cells, $Ca_v1.2$ (α_{1H}), β_2, and ahnak form a stable complex, allowing for cytoskeleton independent Ca^{2+} signaling (Shao et al., 2009).

1.5.4 γ subunit

There are eight different genes that encode for the 35 kDa γ subunit. It is an accessory glycoprotein that is heavily glycosylated with four transmembrane segments and intracellular N- and C- termini. The γ subunit may function to alter the gating characteristics of VSCCs (Catterall, 2000). The γ subunit can downregulate VSCC activity by hyperpolarizing the membrane voltage (Black, 2003). The γ subunit most likely does not affect channel assembly and trafficking (Arikkath and Campbell, 2003).

The γ_1 subunit is primarily expressed in skeletal tissue, while $\gamma_{2,}$ $\gamma_{4,}$ $\gamma_{5,}$ γ_6, and γ_7 are ubiquitously expressed. γ_3 is predominantly in brain, and γ_8 is found in fetal brain tissue (Burgess et al., 2001). In rodent osteoblastic cells, the known γ subunits were not expressed at any stage of development (Bergh et al., 2003). In rabbit brain, γ_2 and γ_3 were shown to associate with the α_{1A} and α_{1B} subunits (Kang et al., 2001), and in mouse brain, $\gamma_{2,}$ γ_3, and γ_4 associated with the α_{1B} subunit (Sharp et al., 2001).

1.6 Goals and Specific Aims

A major public concern, osteoporosis compromises bone strength, leading to an increased susceptibility to fracture. The mechanism underlying the pathology has yet to be completely understood. However, the effect of osteoporosis on the remodeling process permits a cellular explanation. Osteocytes, known to sense strain and transmit signals, are actively involved in the remodeling process, and play a

crucial role in mechanotransduction. In osteoblasts, it has been shown that the VSCCs play an important role in mechanosensation. These cells predominantly express the T-type $Ca_v1.2$ (α_{1C}) VSCCs, while osteocytes express the T-type $Ca_v3.2$ (α_{1H}) subunit more abundantly. While there is evidence to suggest that VSCCs are vital for bone remodeling, the exact composition of the T-type structure has not been elucidated in osteocytes. **My hypothesis is that the $\alpha_2\delta$ subunit is present in MLO-Y4 cells and it associates with the $Ca_v3.2$ subunit to form a VSCC complex in mechanosensitive osteocytes.** In order to carry out this study, two specific aims were devised. The first was to identify the presence of auxiliary subunit transcripts in MLO-Y4 cells. The second aim was to detect the presence of auxiliary protein to ultimately identify the complex association between the T-type $Ca_v3.2$ (α_{1H}) subunit and the $\alpha_2\delta_1$ subunit.

Chapter 2

MATERIALS AND METHODS

2.1 Cell Culture

MLO-Y4 cells, a gift from Dr. Lynda Bonewald, were grown in cell culture in alpha minimal essential media (α-MEM) (GIBCO, NY, NY) containing L-glutamine, ribonucleosides and deoxyribonucleosides with fetal bovine serum (FBS) (2.5%, v/v) (JRH Laboratories, Lenexa, Kansas), and penicillin/streptomycin (1%, v/v). MLO-Y4 cells were cultured on 100mm plates coated with rat tail type I collagen (0.15 mg/mL) (BD Biosciences, Bedford, MA) coated plates. Cells were grown to approximately 80 percent confluency and total RNA extracts were obtained.

2.2 RNA extraction

Total RNA extracts were obtained from MLO-Y4 using the RNeasy Mini Kit (Qiagen, Valencia, CA). Briefly, cells were washed three times with phosphate buffered saline (PBS), lysed in the presence of β-mercaptoethanol, homogenized, and RNA purified using RNeasy columns. To remove residual genomic DNA, the DNA-free DNase Treatment kit was used (Ambion Inc., Austin, TX). 10X DNase I Buffer and rDNase I were added to the mRNA, which was then incubated for 30 minutes at

37°C. The DNase Inactivation Reagent was then added to the mixture, followed by incubation, centrifugation, and RNA transfer. Extracts were stored at -80°C until use.

2.3 Reverse Transcriptase-Polymerase Chain Reaction (RT-PCR)

OmniScript® reverse transcriptase kit was used to obtain a cDNA template from MLO-Y4 RNA extracts (Qiagen, Valencia, CA). The reaction was carried out according to the manufacturers protocol with the addition of Recombinant RNasin® Ribonuclease Inhibitor (Promega, Madison, WI) and random hexamers (Qiagen, Valencia, CA). The final mixture then was incubated for 60 minutes at 37°C. Total mouse embryo mRNA, which was used as a positive control, also was reverse transcribed using the OmniScript® reverse transcriptase kit.

PCR was performed using the GoTAQ® Green PCR kit (Promega, Madison, WI). GoTAQ® Green Master Mix (50%), forward and reverse primers (4%), and cDNA template (10%) were added to a total volume of 25µL per reaction.

The settings for the thermal cycler are as follows: 95°C for 15 minutes, then 35 cycles of 94°C for 30 seconds, 60°C for 30 seconds, 72°C for 1 minute, and then 72°C for 10 minutes, followed by holding at 4°C.

Each primer was custom designed using the transcript sequence obtained from the NCBI database (http://www.ncbi.nlm.nih.gov, 5-28-2009). Transcript sequences were copied to the Biology workbench database (University of California San Diego) to create each primer (http://workbench.sdsc.edu, 5-28-2009). Sequence specificity

was verified using NCBI basic local alignment search tool (BLAST) database (http://blast.ncbi.nlm.nih.gov/Blast.cgi, 5-28-2009). To ensure low heterodimerization and homodimerization of each primer, the oligoanalyzer tool from Integrated DNA technologies database was used (http://www.idtdna.com/analyzer/Applications/OligoAnalyzer, 5-28-2009).

Finally, PCR products were sequenced and compared to known transcript sequences from the NCBI database to validate primer specificity.

Table 2: Primer set information. VSCC subunit primer set information is shown in sections A-D, with positive control sequences in E. The sequence, accession number, and PCR product size are all shown. Panel A shows the α_1 subunits, Panel B shows the β subunits, Panel C shows the $\alpha_2\delta$ subunits, Panel D shows the γ subunits, while Panel E displays the β-actin and E11 sequences. Forward primers are denoted by F and reverse primers are denoted by R.

A.

mRNA	Accession Number	Sequence	Product Size (bp)
$Ca_v1.1(\alpha_{1S})$ F	NM_014193	5'-ACAACCCAGTGTTTTCCAGC-3'	290
$Ca_v1.1(\alpha_{1S})$ R		5'-GTGCTCCTCAAAGTTCCTGC-3'	
$Ca_v1.2(\alpha_{1c})$ F	NM_009781	5'-GTGGTTAGCGTGTCCCTCAT-3'	413
$Ca_v1.2(\alpha_{1c})$ R		5'-GTGGAGACGGTGAAGAGAGC-3'	
$Ca_v1.3(\alpha_{1D})$ F	NM_028981	5'- GTTGCCGTTGACTTTGGTTT -3'	353
$Ca_v1.3(\alpha_{1D})$ R		5'- TGAAAACTTCAGCCCTTGCT -3'	
$Ca_v1.4(\alpha_{1F})$ F	NM_19582	5'- TTTGACTGCTTCGTGGTCTG-3'	540
$Ca_v1.4(\alpha_{1F})$ R		5'- CTCTCTGCCCTTGTCTTTGG-3'	
$Ca_v2.1(\alpha_{1A})$ F	NM_007578	5'-CTGCTTTGAAGAGGGGACAG-3'	284
$Ca_v2.1(\alpha_{1A})$ R		5'-AAAAGGAGCCGATGATGATG -3	
$Ca_v2.2(\alpha_{1B})$ F	NM_001042528	5'- TGAGCGACTAGATGACACGG-3'	397
$Ca_v2.2(\alpha_{1B})$ R		5'- ATCTGTGCTGTTGGGGAAAC-3'	
$Ca_v2.3(\alpha_{1E})$ F	NM_009782	5'-GACAGTGGGAGGGAATCAGA-3'	334
$Ca_v2.3(\alpha_{1E})$ R		5'-CAGGGGTTCTTGTCTGGTGT-3'	
$Ca_v3.1(\alpha_{1G})$ F	NM_009783	5'- TGAGGTCAATGCTTCACTGC-3'	376
$Ca_v3.1(\alpha_{1G})$ R		5'- GGTGGACTCCTGGTCACAGT-3'	
$Ca_v3.2(\alpha_{1H})$ F	NM_021415	5'- TGACAGTGGAGATGAGCCTG-3'	516
$Ca_v3.2(\alpha_{1H})$ R		5'- GAAGGATGCCGAGTGATGAT-3'	
$Ca_v3.3(\alpha_{1I})$ F	NM_001044308	5'-ACCAGAAGAGGACGACGAGA-3'	571
$Ca_v3.3(\alpha_{1I})$ R		5'-CTTGCGAAGGATGTGACAGA-3'	

B.

mRNA	Accession Number	Sequence	Product Size (bp)
β_1 F	NM_145121	5'-AGCATGCCAGTGTGCACGAGTAC-3'	400
β_1 R		5'-AGCCCTCCAGCTCATTCTTATTGC-3'	
β_2 F	NM_023116	5'-ATAACCACAGAGAGGAGACCCACA-3'	220
β_2 R		5'-TATACATCCCTGTTCCACTCGCCA-3'	
β_3 F	NM_007581	5'-TCCCTGGACTTCAGAACCAGCAG-3'	290
β_3 R		5'-TTGTGGTCATGCTCCGAGTCCTG-3'	
β_4 F	NM_001037099	5'-GAGAGCGAAGTCCAAACCTG-3'	473

β_4 R		5'- CAAAGAGGGCTTTCTGCATC-3'	

C.

mRNA	Accession Number	Sequence	Product Size (bp)
$\alpha_2\delta_1$ F	NM_009784	5'- ATACACATGGACGCCTGTCA -3'	408
$\alpha_2\delta_1$ R		5'- CTCGTAATCCCACCGTCTGT -3'	
$\alpha_2\delta_2$ F	NM_020263	5'- ACCTGTACGATGTCCGAAGG -3'	552
$\alpha_2\delta_2$ R		5'- CGATGGAAGGGATCTCAAAA -3'	
$\alpha_2\delta_3$ F	NM_009785	5'- GTGTGGTTGGCACAGATGTC -3'	570
$\alpha_2\delta_3$ R		5'- TGTCACATTGAAGCAGAGGC -3'	
$\alpha_2\delta_4$ F	NM_001033382	5'-ACAGGCAGAGGGAGAGACAA-3'	549
$\alpha_2\delta_4$ R		5'-TGTGTGTTCACTTGGGCATT-3'	

D.

mRNA	Accession Number	Sequence	Product Size (bp)
γ_1	NM_007582	5'-CACCCACACCTCAACGACC-3'	486
γ_1		5'-CCTGCGAAGGCATAAAACAT-3'	
γ_2	NM_007583	5'-CAGAAGTCGGTTGGGTGTTT-3'	376
γ_2		5'-AGGATCACACTCAGGATCGG-3'	
γ_3	NM_019430	5'- ATCCTCAGCGTCACTCTGCT -3'	390
γ_3		5'-GCGAGAACTTGACCGTCTTC -3'	
γ_4	NM_019431	5'-AGGATCTACAGCCGCAAGAA-3'	362
γ_4		5'-GACCTTGAACTGGACCTGGA-3'	
γ_5	NM_080644	5'- CCACAGAACCAGAGCACAGA-3'	420
γ_5		5'- AGCAAAGGCAAATGACCATC-3'	
γ_6	NM_133183	5'-CAGAATCTCGGCTTGACTCC-3'	409
γ_6		5'- GCACCATGATGACACAGAGG-3'	
γ_7	NM_133189	5'- ACGGCTACACCCTTCCCTAT-3'	389
γ_7		5'- GAGTAGTCGGAGCAGTCGCT-3'	
γ_8	NM_133190	5'- AGAGAGGGGTTTGTGGTGTG-3'	316
γ_8		5'- GTGGTCGTAGTCCGTGTCCT-3'	

E.

mRNA	Accession Number	Sequence	Product Size (bp)
β-actin F	NM_007393	5'- TGTTACCAACTGGGACGACA-3'	573
β-actin R		5'- AAGGAAGGCTGGAAAAGAGC-3'	
E11 F	NM_010329	5'- GTGACCCCAGGTACAGGAGA-3'	428
E11 R		5'- GCTCTTTAGGGCGAGAACCT-3'	

2.4 Agarose Gel Electrophoresis

Following the PCR reaction, agarose gel electrophoresis was used to separate amplification products.

Briefly, products were separated using agarose (1.5%, w/v) (Fisher Scientific, Pittsburgh, PA) in Tris-Acetate-ethylene diamine tetraacetic acid (EDTA) (TAE) with ethidum bromide (0.4mg/mL). Approximately 1.2µg of product were loaded into each well. The O'GeneRuler 50bp DNA Ladder (0.1µg/µL) (Fermentas, Glen Burnie, MD) was used as a size marker. Gels were subjected to electrophoresis at 90V for approximately 1 hour, and viewed using an Alpha Imager UV bed and image capture system (Alpha Innotech, San Leandro, CA).

2.5 Western Blotting

MLO-Y4 cells were cultured as previously mentioned, then scraped from the culture, and solubilized with Sample Extraction Buffer (SEB). Extracts were precipitated with trichloroacetic acid (TCA) and the protein concentration was determined using the Lowry Protein Assay. Protein extracts were separated on a 4-12% Bis-Tris NuPage Polyacrylamide gel (Invitrogen, Carlsbad, CA) and transferred to a nitrocellulose membrane at 40V for 5 hours at 4°C. The membrane was blocked overnight at 4°C in 5% milk in tris-buffered saline (TBS) with 0.1% Tween-20. Primary antibody dilutions are as follows: $Ca_v3.1$ (α_{1G}) rabbit polyclonal (Santa Cruz Biotechnology, Inc, Santa Cruz, CA) 1:200, $Ca_v3.2$ (α_{1H}) rabbit polyclonal (Bethyl

Labs, Inc, Montgomery, TX) 1:5000, $\alpha_2\delta_1$ mouse monoclonal [20A] (Abcam®, Cambridge, MA) 1:500. After primary antibodies were added, the blots oscillated at room temperature for 2 hours, and then were washed with TBS-T. Next, a 1:1,000 dilution of horseradish-peroxidase (HRP) conjugated goat anti-rabbit and rabbit anti-mouse were added to the blots for 1 hour at room temperature with oscillation. After a final wash with TBS-T, SuperSignal® West Dura Extended Duration Substrate (Pierce, Rockford, IL) was added and bands were visualized using a X-OMat autoradiography film developer (Kodak®, Rochester, NY) to visualize the immunoreactive bands.

2.6 Immunocytochemistry

MLO-Y4 (2000) cells were seeded into 8-well chambers (NUNC™, Rochester, NY) and cultured under previously described conditions until they reached 85% confluency as judged by eye. Cells were washed with TBS and fixed with 4% paraformaldehyde (EMS, Hatfield, PA) in TBS. Cells then were washed with TBS to remove any remaining fixative and then incubated for 1 hr. with a blocking solution consisting of bovine serum albumin (BSA) (3%, w/v) and normal serum (10%, v/v) from the species in which the required secondary antibody was raised. Antigen specific primary antibodies were added after blocking, and incubated for 1 hr. at RT. Primary antibodies were diluted as follows: $Ca_v3.2$ (α_{1H}) rabbit polyclonal (Bethyl Labs, Inc, Montgomery, TX) 1:100, $\alpha_2\delta_1$ rabbit polyclonal (provided by Dr. Jesús García, created by Bethyl Labs, Inc, Montgomery, TX) 1:50. Following incubation with the primary

antibody, cells were washed with blocking solution and incubated with species specific Alexa Fluor®-conjugated (Invitrogen™, Carlsbad, CA) secondary antibodies (1:200). The secondary antibody solution contained DRAQ5™ nuclear stain (1:1000) (Biostatus, Ltd, Shepshed Leicestershire, United Kingdom). Cells were washed, mounted, and stored at 4°C until imaged with the Zeiss LSM 510 VIS confocal microscope (Zeiss, Inc, Thornwood, NY).

2.7 Co-Immunoprecipitation

Five plates (100 mm) of MLO-Y4 osteocyte-like cells were cultured to approximately 80% confluence and lysed with lysis buffer containing CHAPS (1%, w/v), KCl (300 mM), NaCl (150 mM), sodium phosphate buffer (10 mM, pH 7.4), and protease inhibitor cocktail set (PICS) (1:100). The total cell lysates were scraped from the first plate and added to each plate thereafter to create a final combined lysate.

Lysates were precleared with anti-rabbit IgG beads (50 µl) (eBioscience™, San Diego, CA) and then incubated on ice for 30 min. The lysate/IgG bead mixture then was centrifuged at 10,000g for 3 minutes and the supernatant was transferred to a new tube. Rabbit anti-$Ca_v3.2$ (α_{1H}) (5 µg) was added to the precleared lysates and samples incubated on ice for 1 hour Anti-rabbit IgG beads (50 µl) were added to the lysate/Ab mixture and incubated at 4°C for 1 hour. The mixture then was centrifuged at 10,000g for 1 minute followed by complete removal of the supernatant from the beads. Beads were washed with lysis buffer containing PICS (1:100) and centrifuged at 10,000g for

1 minute after each wash and the wash supernatants were used for Western blot analysis. Laemmli buffer (BioRad, Hercules, CA) with βMercaptoethanol (βME) (2.0%, v/v) was added to the samples, followed by boiling for ten minutes. The assay was completed as previously described using the mouse anti-$\alpha_2\delta_1$ monoclonal antibody to probe for the $\alpha_2\delta_1$ subunit pulled down with the $Ca_v3.2$ (α_{1H}) subunit.

Chapter 3

RESULTS

3.1 Detection of VSCC accessory subunit transcripts

RT-PCR was performed to assess the mRNA expression of the VSCC auxiliary subunits expressed in MLO-Y4 cells (Figure 4). Using subunit specific primers, the results showed that the osteocyte like MLO-Y4 cells expressed $\alpha_2\delta_1$ subunit transcript, but not $\alpha_2\delta_2$, $\alpha_2\delta_3$, or $\alpha_2\delta_4$. Transcripts encoding β_1 subunits were expressed, with β_2 and β_3 present in lesser amounts. No β_4 subunit transcript was detected. Interestingly, the mRNA transcript for γ_7 was expressed; however, no $\gamma_{1\text{-}6,8}$ transcript was detected. There were four controls used for the RT-PCR experiments. β-actin, a highly conserved component of the cytoskeleton, was used as a positive control. In addition, E11, an osteocytic marker, was used as a positive control. All VSCC auxiliary subunits successfully detected both positive controls. One of the negative controls was MLO-Y4 mRNA without reverse transcriptase added (-RT) and the other was sample without any genetic material, only water. As expected, all samples did not demonstrate any banding for the negative controls.

Visual estimates of signal intensity were made to semi-quantify transcript expression levels for all accessory subunits (Table 3; B, C, D). Total mouse embryo

(TME) was used as a positive control because it is known to express all of the investigated subunits. Bands for each of the subunits in MLO-Y4 cells were compared to the bands for the TME positive controls, and relative to the intensity, the bands were assigned either +, ++, +/- or -. The results reflect the patterns described above.

3.2 Detection of α_1 subunit transcripts

The transcript expression of the four α_1 subunit families was investigated through the use of RT-PCR (Figure 5). Of the four members of the Ca_v1 family, only trace amounts of $Ca_v1.2$ were expressed; $Ca_v1.1$, $Ca_v1.3$, and $Ca_v1.4$ were not expressed. MLO-Y4 cells did not express any of the P/Q-, R-, or N-type subunits. Furthermore, two subunits from the T-type Ca_v3 family were expressed. $Ca_v3.2$ (α_{1H}) was detected at higher levels compared to $Ca_v3.1$ (α_{1G}). The relative expression of the pore-forming α_1 subunit compared to transcript expression in TME was also demonstrated; mirroring the patterns described above (Table 3; A).

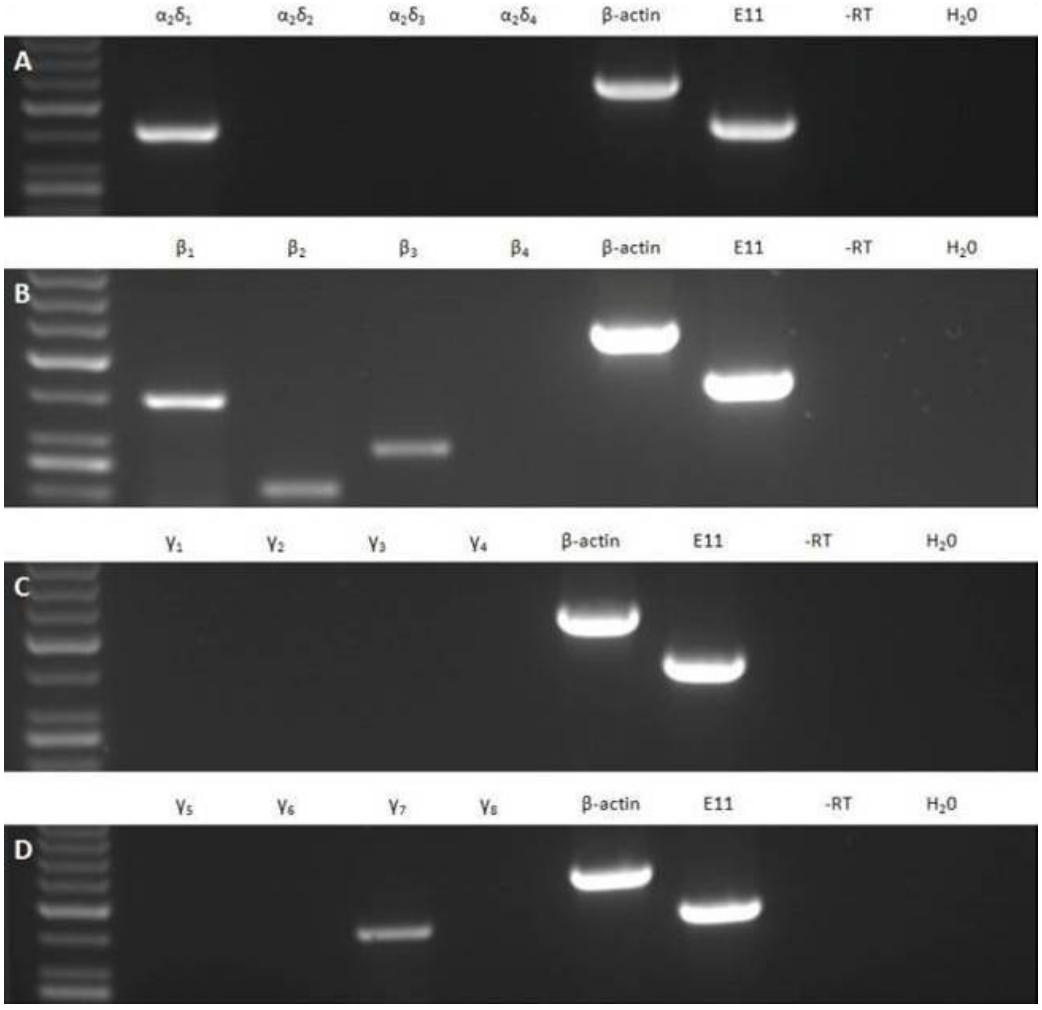

Figure 4: Expression of the auxiliary subunits in MLO-Y4 cells. Panel A shows $\alpha_2\delta$ expression, Panel B shows β expression, and Panels C and D show the γ subunits. β-actin and E11 are positive markers for osteocytes and the –RT and H_2O lanes are negative controls.

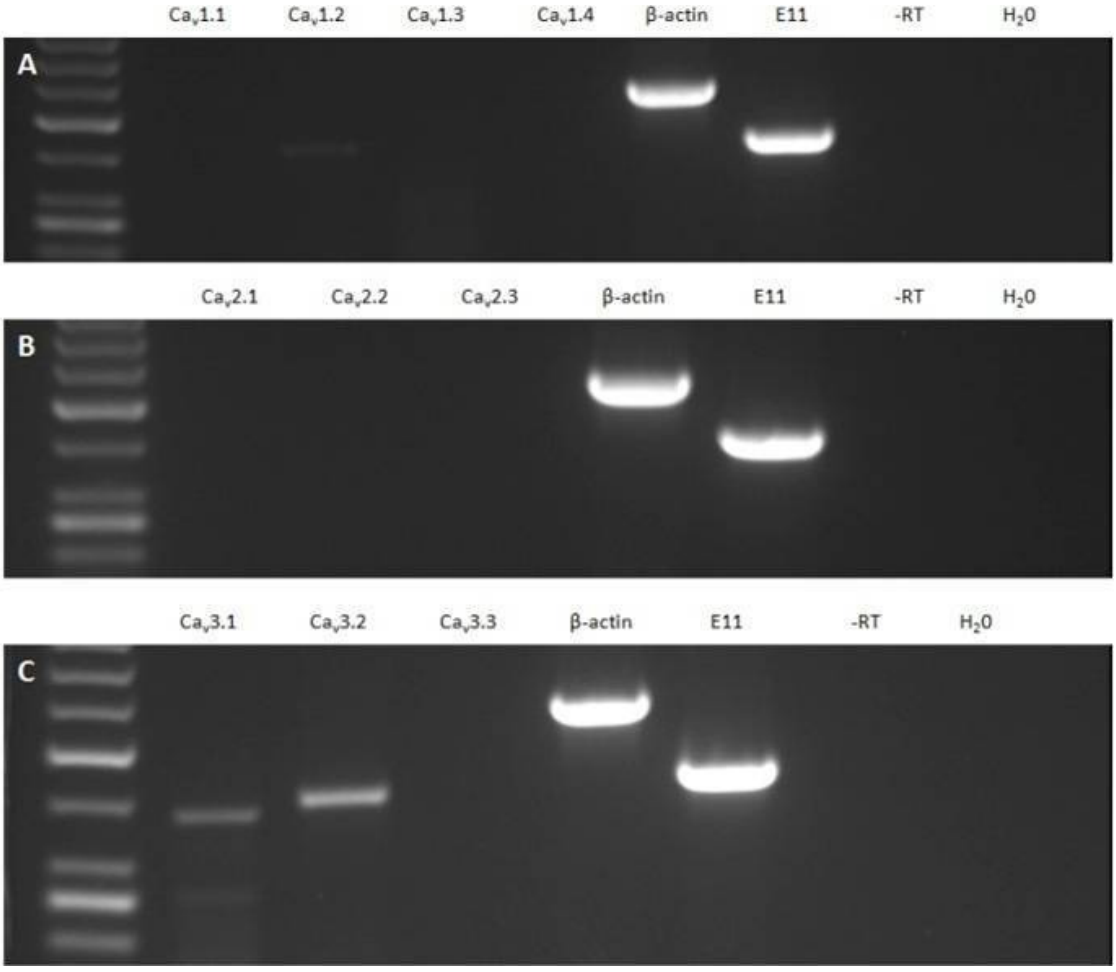

Figure 5: Expression of the α_1 subunit in MLO-Y4 cells. Panel A shows the L-type VSCC expression, Panel B shows the P/Q-, R-, and N-type subunits, and Panel C shows the T-type subunits. β-actin and E11 are positive markers for osteocytes and the –RT and H_2O lanes are negative controls.

Table 3: mRNA expression of VSCC subunits in MLO-Y4 cells relative to TME through the use of RT-PCR. + signifies that it is expressed less than TME, ++ means that it is expressed at the same level as TME, +/- means that it is a very light band, and – means that it is not present. Panel A shows α_1 data, Panel B shows β subunit data, Panel C shows $\alpha_2\delta$ data, and Panel D shows γ subunit data.

A.

Current Type	Subunit	Transcript
L-type	α_{1S}	-
	α_{1C}	+/-
	α_{1D}	-
	α_{1F}	-
P/Q-type	α_{1A}	-
N-type	α_{1B}	-
R-type	α_{1E}	-
T-type	α_{1G}	+
	α_{1H}	+
	α_{1I}	-

B.

Subunit	Transcript
β_1	++
β_2	+
β_3	+
β_4	-

C.

Subunit	Transcript
$\alpha_2\delta_1$	++
$\alpha_2\delta_2$	-
$\alpha_2\delta_3$	-
$\alpha_2\delta_4$	-

D.

Subunit	Transcript
γ_1	-
γ_2	-
γ_3	-
γ_4	-
γ_5	-
γ_6	-
γ_7	+
γ_8	-

3.3 Protein detection of α_{1H} and $\alpha_2\delta_1$

Western blotting was performed to validate the mRNA studies in relation to the protein expression of the channel subunits (Figure 6). $Ca_v3.2$ (α_{1H}) protein was detected in MLO-Y4 cells. However, the T-type $Ca_v3.1$ (α_{1G}) subunit was not detected through western blotting. Due to the availability of skeletal muscle (Sk. mm) protein, this was used as the positive control for both T-type protein blots. Protein for the auxiliary $\alpha_2\delta_1$ subunit was demonstrated in MLO-Y4 cells in a higher amount compared to $Ca_v3.2$ (α_{1H}). Skeletal muscle was used as a positive control because the antibody used for the detection of $\alpha_2\delta_1$ was optimized for use in rat skeletal muscle.

Immunohistochemical studies also were performed to localize channel subunits to the MLO-Y4 cells. Immunostaining of α_{1H} and $\alpha_2\delta_1$ clearly was observed in MLO-Y4 cells (Figure 6, Figure 7). The α_{1H} subunit exhibited well-defined staining along the membrane in addition to within the dendrite-like extensions projecting from the cell body. There were two negative controls used; one with rabbit IgG instead of primary antibody to diminish specific staining and the other with application of the secondary antibody only. Additionally, MLO-Y4 cells were probed with a mouse anti-$\alpha_2\delta_1$ antibody. The $\alpha_2\delta_1$ subunits were found to be distributed along the plasma membrane with a large amount of intracellular staining. Two negative controls were used; one with rabbit IgG and the other with secondary only.

A. $Ca_v3.2$ (α_{1H})

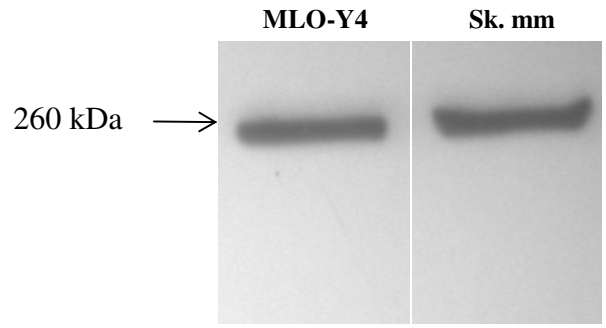

B. $Ca_v3.1$ (α_{1G})

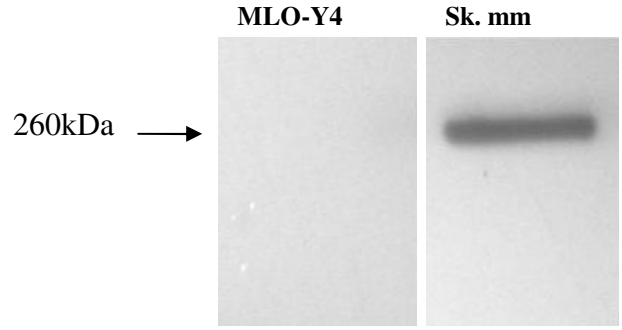

C. $\alpha_2\delta_1$

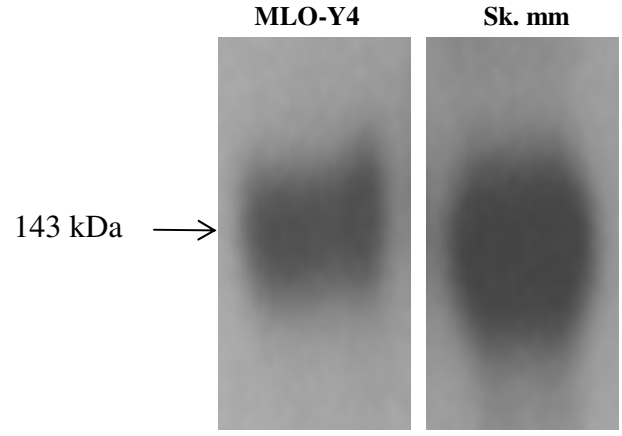

Figure 6: Western blotting results in MLO-Y4 cells. A) Presence of $Ca_v3.2$ (α_{1H}) protein. B) $Ca_v3.1$ (α_{1G}) protein is not expressed. C) Presence of the $\alpha_2\delta_1$ auxiliary subunit. Skeletal muscle (Sk. mm) is the positive control.

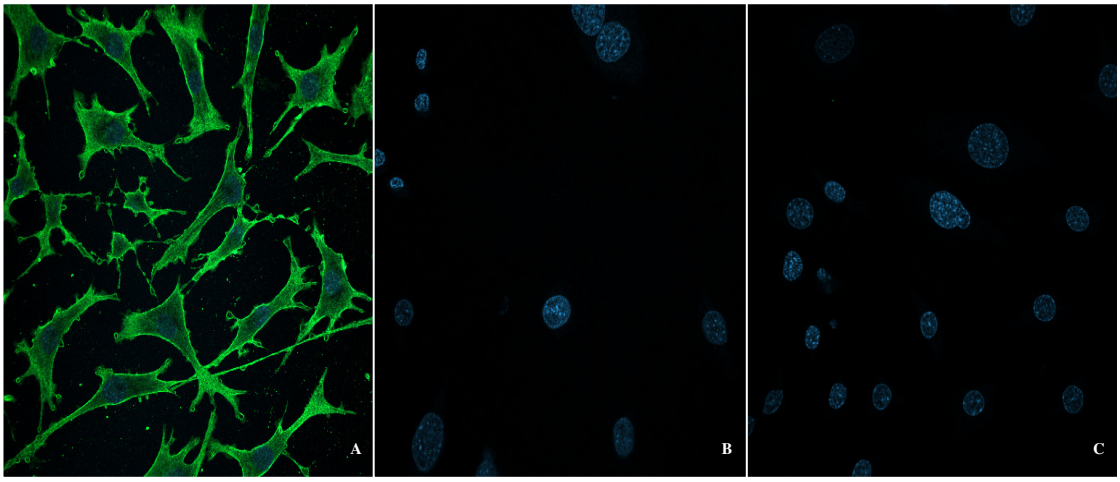

Figure 7: $Ca_v3.2$ (α_{1H}) is present along the membrane of MLO-Y4 cells. Panel A shows staining of MLO-Y4 cells with rabbit polyclonal α_{1H} antibody. Panel B shows the rabbit IgG negative control and Panel C displays the secondary only negative control.

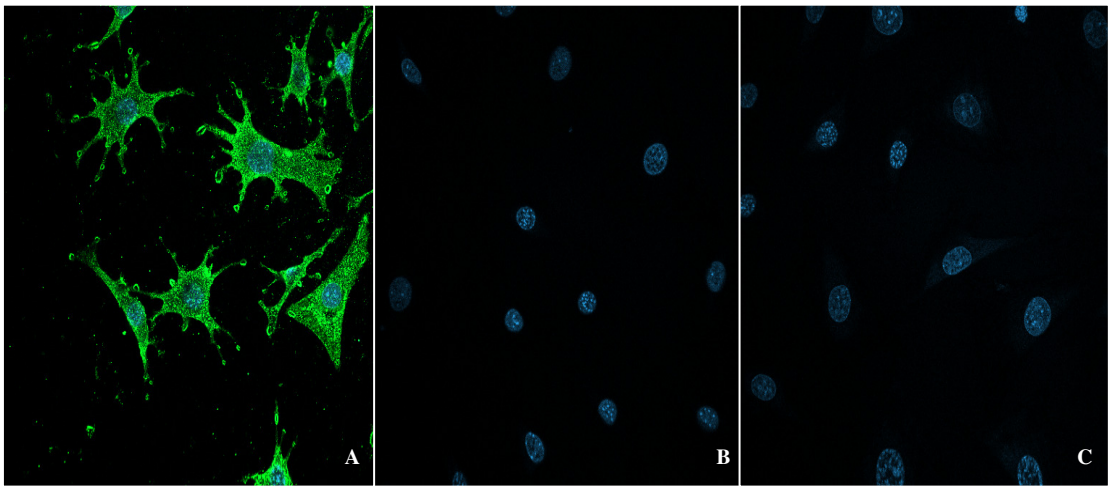

Figure 8: $\alpha_2\delta_1$ is present in the cytoplasmic extensions of MLO-Y4 cells. Panel A shows staining of MLO-Y4 cells with rabbit polyclonal $\alpha_2\delta_1$ antibody. Panel B shows the rabbit IgG negative control and Panel C displays the secondary only negative control.

3.4 T-type $Ca_v3.2$ (α_{1H}) associates with $\alpha_2\delta_1$

To determine if the $\alpha_2\delta_1$ subunit forms an association with the $Ca_v3.2$ (α_{1H}) subunits in MLO-Y4 cells, co-immunoprecipitation and western blotting were performed. If the $\alpha_2\delta_1$ subunit interacted with the pore forming α_{1H} subunit, then it was expected to co-immunoprecipitate with the anti-$Ca_v3.2$ (α_{1H}) antibody and anti-rabbit IgG beads. The results revealed that the auxiliary $\alpha_2\delta_1$ subunit co-precipitated with the $Ca_v3.2$ (α_{1H}) subunits from the total protein extracts of MLO-Y4 cells (Figure 9). The cell lysate was loaded in the first lane. The bead/antibody/lysate mixture was washed three times, and these samples were loaded as well (wash #1, 2, 3). Finally, the eluant, which contained the bound antibody, was loaded in the final column. The negative control for this experiment involved the application of non-immune mouse IgG instead of $\alpha_2\delta_1$. As expected, no co-immunoprecipitation was observed, demonstrating the specificity.

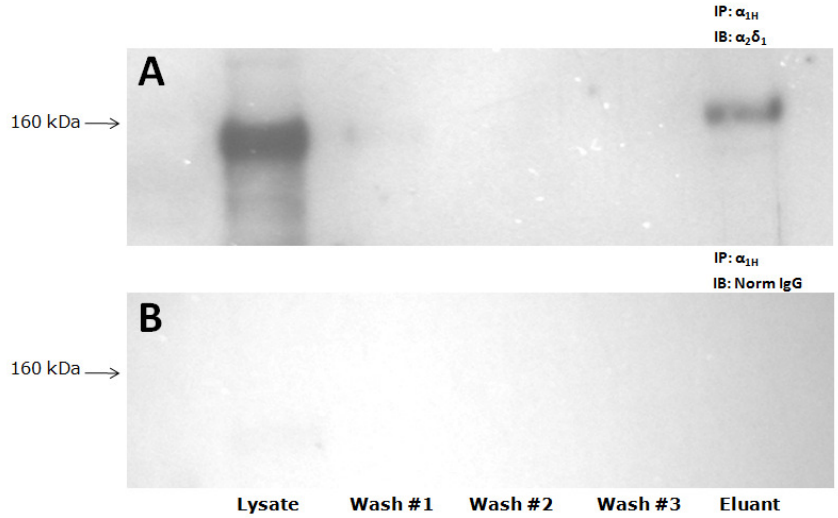

Figure 9: α_{1H} forms a complex with $\alpha_2\delta_1$ in MLO-Y4 cells. The cells were precipitated with Rabbit α_{1H} antibody and blotted with mouse monoclonal $\alpha_2\delta_1$ antibody. Panel A displays the presence of α_{1H} when the blot was blotted with $\alpha_2\delta_1$ antibody indicating their association. Panel B shows the normal mouse IgG control blot. (performed with William Thompson).

Chapter 4

DISCUSSION

4.1 T-type VSCCs in osteocyte-like MLO-Y4 cells express γ_7 transcript

Ca^{2+} ions are secondary messenger molecules that elicit a number of cellular processes, including muscle contraction, neurotransmitter release, secretion, and gene expression (Catterall, 2000). VSCCs serve as the means through which Ca^{2+} enters the cell, and they are composed of a variety of subunits, which regulate channel assembly, trafficking, and gating properties (Catterall, 2000). While there have been a number of studies investigating VSCCs, the subunit composition of T-type VSCCs remains incompletely understood (Perez-Reyes, 2006).

The α_{1H} subunit determines the fundamental properties of VSCCs and has been implicated as a target for phosphorylation, emphasizing its integral role in channel function (Catterall, 2000). In this study, I demonstrated by RT-PCR, the trace appearance of $Ca_v1.2$ (α_{1C}) transcript, an L-type channel. In addition, I found higher levels of two T-type channel transcripts, $Ca_v3.1$ (α_{1G}) and $Ca_v3.2$ (α_{1H}) in MLO-Y4 cells. In agreement with previous studies, the $Ca_v3.2$ (α_{1H}) subunit was expressed in MLO-Y4 cells. Immunostaining revealed the localization of the α_{1H} subunit to the membrane of MLO-Y4 cells. Interestingly, osteoblasts, which are osteocyte precursors,

express the L-type $Ca_v1.2$ (α_{1C}) subunit as the most prevalent type of calcium channel (Meszaros et al., 1996). Considering the predecessor of osteocytes, the presence of trace amount of $Ca_v1.2$ is not surprising. However, it is important to note that there is a shift from the L-type expressing osteoblasts to the T-type expressing osteocytes. The presence of the T-type $Ca_v3.2$ subunit in MLO-Y4 cells provides a mechanism whereby osteocytes can respond by membrane depolarization and possibly by the modulation of auxiliary subunits. Despite the presence of α_{1G} transcript, protein was not detected, for the $Ca_v3.1$ (α_{1G}) subunit. A possible explanation for the absence of the α_{1G} protein is that post-transcriptional processes may have resulted in degradation of the α_{1G} mRNA.

Like osteoblasts, MLO-Y4 osteocytes express the $\alpha_2\delta_1$ transcript in addition to β_1, β_2, and β_3 subunit transcripts. The latter finding could suggest the presence of multiple β subunit proteins, providing for greater diversity in VSCC activity. The α_1-β association is important for cellular trafficking of the α_1 subunit to the plasma membrane (Bichet et al., 2000). Bergh and colleagues have demonstrated that osteoblasts do not express the γ subunit (Bergh et al., 2003). Interestingly, osteocyte-like MLO-Y4 cells showed the presence of the γ_7 transcript. While the γ subunit does not confer functions relating to channel assembly, it is associated with electrical excitability and has been shown to alter gating properties (Catterall, 2000, Arikkath and Campbell, 2003, Black, 2003). Presently, eight subunit subtypes ($\gamma_{1\text{-}8}$) have been

characterized, but at the time of the osteoblastic study, only two γ subunits were discovered.

4.2 Association between the T-type α_{1H} subunit and the $\alpha_2\delta_1$ auxiliary subunit

Western blotting of the $\alpha_2\delta_1$ subunit revealed the presence of $\alpha_2\delta_1$ protein in MLO-Y4 cells and immunostaining assays demonstrated that $\alpha_2\delta_1$ is present along the membrane and in the cytoplasm. The association of $\alpha_2\delta_1$ with the α_1 subunit could increase the current peak amplitude and channel activation/inactivation rate (Singer et al., 1991, Williams et al., 1992). Numerous studies have attempted to demonstrate an association of auxiliary VSCC subunits with T-type subunits. While previous studies have shown the association between high-voltage activated channels and auxiliary subunits, to date, there is no significant evidence to demonstrate an association between auxiliary subunits and T-type VSCCs (Perez-Reyes, 2006). The novel finding described in this study demonstrates the presence of a complex between T-type $Ca_v3.2$ (α_{1H}) and $\alpha_2\delta_1$. The presence of the von Willebrand factor A domain in extracellular auxiliary $\alpha_2\delta_1$ VSCC subunit on the membrane of osteocyte processes provides an element through which an extracellular physical signal may alter the gating properties of the channel.

The ability of $\alpha_2\delta_1$ to complex with α_{1H} provides the framework for which the extracellular component of $\alpha_2\delta_1$ can project into the pericellular space and interact with the ECM. Garcia and colleagues found that, *in vitro*, the knockdown of $\alpha_2\delta_1$ in

skeletal muscle myoblasts impaired the ability of cells to migrate, attach, and spread, suggesting that $\alpha_2\delta_1$ may play a role in extracellular signaling, a mechanism mediated by the ability of $\alpha_2\delta_1$ to attach to surface-residing matrix molecules (Garcia et al., 2008). The novel role of this subunit as demonstrated above, strengthens the hypothesis that the $\alpha_2\delta_1$ subunit may play a role in ECM interactions.

4.3 Future Work and Conclusions

By understanding the molecular architecture of the T-type VSCC, the potential regulatory sites on these channels can be further studied. The findings from this research project lead to great insight in the composition of the T-type VSCC. Expression of the $\alpha_2\delta_1$ auxiliary subunit in MLO-Y4 cells provides a link between the extracellular environment, where mechanically induced fluid flow events occur, and the intracellular environment, where the T-type $Ca_v3.2$ subunit may alter signaling within bone. By exploring the structure of VSCCs, a more complete understanding of mechanotransduction in osteocytes can be elucidated, potentially assisting in the progression made by pharmaceutical companies in the battle against osteoporosis.

Future work needs to be done to further characterize the T-type Ca^{2+} in MLO-Y4 osteocytes. The β subunit, known to complex with $Ca_v1.2$ (α_{1C}) in osteoblasts is another potential auxiliary subunit of T-type VSCCs in osteocytes. In addition, the presence of the γ_7 indicates the possibility for another auxiliary subunit to be characterized in MLO-Y4 cells.

REFERENCES

1. Cooper C. Epidemiology of osteoporosis. Osteoporos Int 1999;9 Suppl 2:S2-8.

2. Holroyd C, Cooper C, Dennison E. Epidemiology of osteoporosis. Best Pract Res Clin Endocrinol Metab 2008;22:671-685.

3. Johnell O, Kanis JA. An estimate of the worldwide prevalence and disability associated with osteoporotic fractures. Osteoporos Int 2006;17:1726-1733.

4. Miller PD. Management of osteoporosis. Dis Mon 1999;45:21-54.

5. Cummings SR, Melton LJ. Epidemiology and outcomes of osteoporotic fractures. Lancet 2002;359:1761-1767.

6. Aarden EM, Burger EH, Nijweide PJ. Function of osteocytes in bone. J Cell Biochem 1994;55:287-299.

7. Katagiri T, Takahashi N. Regulatory mechanisms of osteoblast and osteoclast differentiation. Oral Dis 2002;8:147-159.

8. Lian JB, Stein GS. Development of the osteoblast phenotype: molecular mechanisms mediating osteoblast growth and differentiation. Iowa Orthop J 1995;15:118-140.

9. Stein GS, Lian JB, Owen TA. Bone cell differentiation: a functionally coupled relationship between expression of cell-growth- and tissue-specific genes. Curr Opin Cell Biol 1990;2:1018-1027.

10. Ash P, Loutit JF, Townsend KM. Osteoclasts derived from haematopoietic stem cells. Nature 1980;283:669-670.

11. Davies J, Warwick J, Totty N, Philp R, Helfrich M, Horton M. The osteoclast functional antigen, implicated in the regulation of bone resorption, is biochemically related to the vitronectin receptor. J Cell Biol 1989;109:1817-1826.
12. Vaananen HK, Zhao H, Mulari M, Halleen JM. The cell biology of osteoclast function. J Cell Sci 2000;113 (Pt 3):377-381.
13. Blair HC. How the osteoclast degrades bone. Bioessays 1998;20:837-846.
14. Marotti G, Ferretti M, Remaggi F, Palumbo C. Quantitative evaluation on osteocyte canalicular density in human secondary osteons. Bone 1995;16:125-128.
15. Wang D, Christensen K, Chawla K, Xiao G, Krebsbach PH, Franceschi RT. Isolation and characterization of MC3T3-E1 preosteoblast subclones with distinct in vitro and in vivo differentiation/mineralization potential. J Bone Miner Res 1999;14:893-903.
16. Knothe Tate ML. "Whither flows the fluid in bone?" An osteocyte's perspective. J Biomech 2003;36:1409-1424.
17. Bonewald LF. Establishment and characterization of an osteocyte-like cell line, MLO-Y4. J Bone Miner Metab 1999;17:61-65.
18. Hadjidakis DJ, Androulakis, II. Bone remodeling. Ann N Y Acad Sci 2006;1092:385-396.
19. Udagawa N, Takahashi N, Akatsu T, Tanaka H, Sasaki T, Nishihara T et al. Origin of osteoclasts: mature monocytes and macrophages are capable of differentiating into osteoclasts under a suitable microenvironment prepared by bone marrow-derived stromal cells. Proc Natl Acad Sci U S A 1990;87:7260-7264.

20. Lacey DL, Timms E, Tan HL, Kelley MJ, Dunstan CR, Burgess T et al. Osteoprotegerin ligand is a cytokine that regulates osteoclast differentiation and activation. Cell 1998;93:165-176.

21. Hofbauer LC, Gori F, Riggs BL, Lacey DL, Dunstan CR, Spelsberg TC et al. Stimulation of osteoprotegerin ligand and inhibition of osteoprotegerin production by glucocorticoids in human osteoblastic lineage cells: potential paracrine mechanisms of glucocorticoid-induced osteoporosis. Endocrinology 1999;140:4382-4389.

22. Lanyon LE. Osteocytes, strain detection, bone modeling and remodeling. Calcif Tissue Int 1993;53 Suppl 1:S102-106; discussion S106-107.

23. Weinbaum S, Cowin SC, Zeng Y. A model for the excitation of osteocytes by mechanical loading-induced bone fluid shear stresses. J Biomech 1994;27:339-360.

24. Skerry TM, Bitensky L, Chayen J, Lanyon LE. Early strain-related changes in enzyme activity in osteocytes following bone loading in vivo. J Bone Miner Res 1989;4:783-788.

25. Raab-Cullen DM, Thiede MA, Petersen DN, Kimmel DB, Recker RR. Mechanical loading stimulates rapid changes in periosteal gene expression. Calcif Tissue Int 1994;55:473-478.

26. Gluhak-Heinrich J, Ye L, Bonewald LF, Feng JQ, MacDougall M, Harris SE et al. Mechanical loading stimulates dentin matrix protein 1 (DMP1) expression in osteocytes in vivo. J Bone Miner Res 2003;18:807-817.

27. Zhang K, Barragan-Adjemian C, Ye L, Kotha S, Dallas M, Lu Y et al. E11/gp38 selective expression in osteocytes: regulation by mechanical strain and role in dendrite elongation. Mol Cell Biol 2006;26:4539-4552.

28. Ajubi NE, Klein-Nulend J, Alblas MJ, Burger EH, Nijweide PJ. Signal transduction pathways involved in fluid flow-induced PGE2 production by cultured osteocytes. Am J Physiol 1999;276:E171-178.
29. Bakker AD, Soejima K, Klein-Nulend J, Burger EH. The production of nitric oxide and prostaglandin E(2) by primary bone cells is shear stress dependent. J Biomech 2001;34:671-677.
30. Tatsumi S, Ishii K, Amizuka N, Li M, Kobayashi T, Kohno K et al. Targeted ablation of osteocytes induces osteoporosis with defective mechanotransduction. Cell Metab 2007;5:464-475.
31. Dolphin AC. The G.L. Brown Prize Lecture. Voltage-dependent calcium channels and their modulation by neurotransmitters and G proteins. Exp Physiol 1995;80:1-36.
32. Catterall WA. Structure and regulation of voltage-gated Ca2+ channels. Annu Rev Cell Dev Biol 2000;16:521-555.
33. Meszaros JG, Karin NJ, Akanbi K, Farach-Carson MC. Down-regulation of L-type Ca2+ channel transcript levels by 1,25-dihyroxyvitamin D3. Osteoblastic cells express L-type alpha1C Ca2+ channel isoforms. J Biol Chem 1996;271:32981-32985.
34. Caffrey JM, Farach-Carson MC. Vitamin D3 metabolites modulate dihydropyridine-sensitive calcium currents in clonal rat osteosarcoma cells. J Biol Chem 1989;264:20265-20274.
35. Bergh JJ, Xu Y, Farach-Carson MC. Osteoprotegerin expression and secretion are regulated by calcium influx through the L-type voltage-sensitive calcium channel. Endocrinology 2004;145:426-436.

36. Perez-Reyes E, Cribbs LL, Daud A, Lacerda AE, Barclay J, Williamson MP et al. Molecular characterization of a neuronal low-voltage-activated T-type calcium channel. Nature 1998;391:896-900.

37. Shao Y, Alicknavitch M, Farach-Carson MC. Expression of voltage sensitive calcium channel (VSCC) L-type Cav1.2 (alpha1C) and T-type Cav3.2 (alpha1H) subunits during mouse bone development. Dev Dyn 2005;234:54-62.

38. Perez-Reyes E. Molecular characterization of T-type calcium channels. Cell Calcium 2006;40:89-96.

39. Perez-Reyes E, Kim HS, Lacerda AE, Horne W, Wei XY, Rampe D et al. Induction of calcium currents by the expression of the alpha 1-subunit of the dihydropyridine receptor from skeletal muscle. Nature 1989;340:233-236.

40. Bergh JJ, Shao Y, Akanbi K, Farach-Carson MC. Rodent osteoblastic cells express voltage-sensitive calcium channels lacking a gamma subunit. Calcif Tissue Int 2003;73:502-510.

41. Arikkath J, Campbell KP. Auxiliary subunits: essential components of the voltage-gated calcium channel complex. Curr Opin Neurobiol 2003;13:298-307.

42. Perez-Reyes E. Molecular physiology of low-voltage-activated t-type calcium channels. Physiol Rev 2003;83:117-161.

43. Burgess DL, Gefrides LA, Foreman PJ, Noebels JL. A cluster of three novel Ca2+ channel gamma subunit genes on chromosome 19q13.4: evolution and expression profile of the gamma subunit gene family. Genomics 2001;71:339-350.

44. Gurnett CA, De Waard M, Campbell KP. Dual function of the voltage-dependent Ca2+ channel alpha 2 delta subunit in current stimulation and subunit interaction. Neuron 1996;16:431-440.

45. Gurnett CA, Felix R, Campbell KP. Extracellular interaction of the voltage-dependent Ca2+ channel alpha2delta and alpha1 subunits. J Biol Chem 1997;272:18508-18512.
46. Jay SD, Sharp AH, Kahl SD, Vedvick TS, Harpold MM, Campbell KP. Structural characterization of the dihydropyridine-sensitive calcium channel alpha 2-subunit and the associated delta peptides. J Biol Chem 1991;266:3287-3293.
47. Ellis SB, Williams ME, Ways NR, Brenner R, Sharp AH, Leung AT et al. Sequence and expression of mRNAs encoding the alpha 1 and alpha 2 subunits of a DHP-sensitive calcium channel. Science 1988;241:1661-1664.
48. Gong HC, Hang J, Kohler W, Li L, Su TZ. Tissue-specific expression and gabapentin-binding properties of calcium channel alpha2delta subunit subtypes. J Membr Biol 2001;184:35-43.
49. Anantharaman V, Aravind L. Cache - a signaling domain common to animal Ca(2+)-channel subunits and a class of prokaryotic chemotaxis receptors. Trends Biochem Sci 2000;25:535-537.
50. Klugbauer N, Marais E, Hofmann F. Calcium channel alpha2delta subunits: differential expression, function, and drug binding. J Bioenerg Biomembr 2003;35:639-647.
51. Helton TD, Horne WA. Alternative splicing of the beta 4 subunit has alpha1 subunit subtype-specific effects on Ca2+ channel gating. J Neurosci 2002;22:1573-1582.
52. Hullin R, Khan IF, Wirtz S, Mohacsi P, Varadi G, Schwartz A et al. Cardiac L-type calcium channel beta-subunits expressed in human heart have differential effects on single channel characteristics. J Biol Chem 2003;278:21623-21630.

53. Liu H, De Waard M, Scott VE, Gurnett CA, Lennon VA, Campbell KP. Identification of three subunits of the high affinity omega-conotoxin MVIIC-sensitive Ca2+ channel. J Biol Chem 1996;271:13804-13810.
54. Dolphin AC. Beta subunits of voltage-gated calcium channels. J Bioenerg Biomembr 2003;35:599-620.
55. Resh MD. Fatty acylation of proteins: new insights into membrane targeting of myristoylated and palmitoylated proteins. Biochim Biophys Acta 1999;1451:1-16.
56. Gao T, Chien AJ, Hosey MM. Complexes of the alpha1C and beta subunits generate the necessary signal for membrane targeting of class C L-type calcium channels. J Biol Chem 1999;274:2137-2144.
57. De Waard M, Pragnell M, Campbell KP. Ca2+ channel regulation by a conserved beta subunit domain. Neuron 1994;13:495-503.
58. Betanzos A, Huerta M, Lopez-Bayghen E, Azuara E, Amerena J, Gonzalez-Mariscal L. The tight junction protein ZO-2 associates with Jun, Fos and C/EBP transcription factors in epithelial cells. Exp Cell Res 2004;292:51-66.
59. Sheng M, Pak DT. Ligand-gated ion channel interactions with cytoskeletal and signaling proteins. Annu Rev Physiol 2000;62:755-778.
60. Takahashi SX, Miriyala J, Colecraft HM. Membrane-associated guanylate kinase-like properties of beta-subunits required for modulation of voltage-dependent Ca2+ channels. Proc Natl Acad Sci U S A 2004;101:7193-7198.
61. Pragnell M, De Waard M, Mori Y, Tanabe T, Snutch TP, Campbell KP. Calcium channel beta-subunit binds to a conserved motif in the I-II cytoplasmic linker of the alpha 1-subunit. Nature 1994;368:67-70.

62. Shao Y, Czymmek KJ, Jones PA, Fomin VP, Akanbi K, Duncan RL et al. Dynamic interactions between L-type voltage-sensitive calcium channel Cav1.2 subunits and ahnak in osteoblastic cells. Am J Physiol Cell Physiol 2009;296:C1067-1078.

63. Black JL, 3rd. The voltage-gated calcium channel gamma subunits: a review of the literature. J Bioenerg Biomembr 2003;35:649-660.

64. Kang MG, Chen CC, Felix R, Letts VA, Frankel WN, Mori Y et al. Biochemical and biophysical evidence for gamma 2 subunit association with neuronal voltage-activated Ca2+ channels. J Biol Chem 2001;276:32917-32924.

65. Sharp AH, Black JL, 3rd, Dubel SJ, Sundarraj S, Shen JP, Yunker AM et al. Biochemical and anatomical evidence for specialized voltage-dependent calcium channel gamma isoform expression in the epileptic and ataxic mouse, stargazer. Neuroscience 2001;105:599-617.

66. Bichet D, Cornet V, Geib S, Carlier E, Volsen S, Hoshi T et al. The I-II loop of the Ca2+ channel alpha1 subunit contains an endoplasmic reticulum retention signal antagonized by the beta subunit. Neuron 2000;25:177-190.

67. Singer D, Biel M, Lotan I, Flockerzi V, Hofmann F, Dascal N. The roles of the subunits in the function of the calcium channel. Science 1991;253:1553-1557.

68. Williams ME, Feldman DH, McCue AF, Brenner R, Velicelebi G, Ellis SB et al. Structure and functional expression of alpha 1, alpha 2, and beta subunits of a novel human neuronal calcium channel subtype. Neuron 1992;8:71-84.

69. Garcia K, Nabhani T, Garcia J. The calcium channel alpha2/delta1 subunit is involved in extracellular signalling. J Physiol 2008;586:727-738.